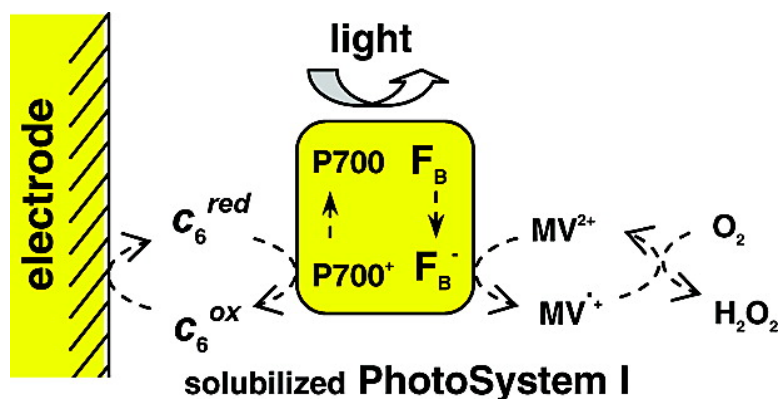


## Electrocatalytic Investigation of Light-Induced Electron Transfer between Cytochrome *c* and Photosystem I

Vanessa Proux-Delrouyre, Christophe Demaille, Winfried Leibl, Pierre Stif, Hervé Bottin, and Christian Bourdillon

*J. Am. Chem. Soc.*, **2003**, 125 (45), 13686-13692 • DOI: 10.1021/ja0363819 • Publication Date (Web): 18 October 2003

Downloaded from <http://pubs.acs.org> on March 30, 2009



### More About This Article

Additional resources and features associated with this article are available within the HTML version:

- Supporting Information
- Links to the 1 articles that cite this article, as of the time of this article download
- Access to high resolution figures
- Links to articles and content related to this article
- Copyright permission to reproduce figures and/or text from this article

[View the Full Text HTML](#)

## Electrocatalytic Investigation of Light-Induced Electron Transfer between Cytochrome $c_6$ and Photosystem I

Vanessa Proux-Delrouyre,<sup>†</sup> Christophe Demaille,<sup>‡</sup> Winfried Leibl,<sup>†</sup> Pierre Sétif,<sup>†</sup> Hervé Bottin,<sup>†</sup> and Christian Bourdillon<sup>\*§</sup>

Contribution from the Service de Bioénergétique, DBJC, CEA Saclay, URA du CNRS N° 2096, 91191 Gif-sur-Yvette, France; Laboratoire d'Electrochimie Moléculaire, UMR du CNRS N°7591, Université Paris 7 - Denis Diderot, 75251 Paris Cedex 05, France; and Laboratoire de Technologie Enzymatique, UMR du CNRS N°6022, Université de Technologie de Compiègne, B. P. 20529, 60205 Compiègne Cedex, France.

Received May 28, 2003; E-mail: Christian.Bourdillon@utc.fr

**Abstract:** A light-activated electron-transfer chain was assembled using solubilized cyanobacterial photosystem I as photoactive enzyme, cytochrome  $c_6$  (also from cyanobacteria) as electron donor, and methyl viologen as electron acceptor. The photocatalytic activity of the ensemble was measured by direct and reversible electrochemistry of cytochrome  $c_6$  at a surface-modified gold electrode. Analysis of the electrochemical response with an appropriate model for the reaction mechanism allowed the relation of the overall catalytic reaction rate to the individual steps of the catalytic cycle. Second-order rate constants were determined for the first time under steady-state conditions. The results validate this approach as an efficient method for the study of electron transfer between photoactive enzymes and their redox partners.

### Introduction:

Intra- and interprotein electron transfers play a fundamental role in bioenergetic reactions such as photosynthesis and respiration. The electron transport chain consists of a series of enzyme complexes, embedded in the membrane, and of small carriers shuttling electrons between them. These electron carriers are lipophilic (e.g., ubiquinone, plastoquinone), laterally mobile in the lipidic core of the membrane, or water soluble (e.g. small cytochromes, plastocyanin, ferredoxin) diffusing along the membrane in the aqueous phase. Cytochrome  $c_6$  (cyt  $c_6$ ) is one of the water-soluble electron carriers involved in the process of photosynthesis in cyanobacteria and green algae;<sup>1</sup> it carries electrons from the cytochrome  $b_6/f$  complex to photosystem I (PSI). Cyt  $c_6$  is now well characterized, and the crystal structure has been described.<sup>2,3</sup> In cyanobacteria, the three-dimensional structure of PSI reveals a complex association of 12 protein subunits (330 kDa) carrying 127 cofactors, mostly chlorophylls.<sup>4</sup> When PSI is illuminated, light absorption generates an excited state of the primary donor P700 followed by electron transfer to the iron–sulfur centers  $F_A$  and  $F_B$  which function as terminal electron acceptors. The successive intraprotein electron transfers in PSI have been well characterized by time-resolved kinetic

studies and occur within less than 1  $\mu$ s after absorption of a photon.<sup>5</sup> The kinetics of electron exchanges with the two natural electron carriers, oxidation of cyt  $c_6$  at the PSI donor side and reduction of ferredoxin at the acceptor side, respectively, have been previously investigated by laser flash absorption spectroscopy.<sup>6,7</sup>

Electrochemical methods offer efficient alternatives for the experimental study of electron transfer between proteins and enzymes. Kinetic measurements using, for example, cyclic voltammetry are based on the coupling between one heterogeneous electrochemical reaction and the catalytic reaction to be studied. The resulting “catalytic current” contains the kinetic information. Following the concept originally developed by Nicholson and Shain,<sup>8</sup> the literature offers several theoretical frameworks now well adapted for the extraction of rate constants from enzymatic electrocatalysis data, either for homogeneous catalysis<sup>9,10</sup> or for direct electron transfer.<sup>11</sup> In the case of light-driven enzymatic electrocatalysis, there are still very few experimental studies,<sup>12</sup> because of the detergent used to stabilize the photosynthetic complexes in solution.<sup>13</sup>

<sup>†</sup> Service de Bioénergétique, DBJC.

<sup>‡</sup> Université Paris 7 - Denis Diderot.

<sup>§</sup> Université de Technologie de Compiègne.

- (1) Kerfeld, C. A.; Krogmann, D. W. *Annu. Rev. Plant Physiol. Plant Mol. Biol.* **1998**, *49*, 397–425.
- (2) Beissinger, M.; Sticht, H.; Sutter, M.; Ejchart, A.; Haehnel, W.; Rösch, P. *EMBO J.* **1998**, *17*, 27–36.
- (3) Kerfeld, C. A.; Sawaya, M. R.; Krogmann, D. W.; Yeates, T. O. *Acta Crystallogr.* **2002**, *D58*, 1104–1110.
- (4) Jordan, P.; Fromme, P.; Witt, H. T.; Klukas, O.; Saenger, W.; Krauss, N. *Nature* **2001**, *411*, 909–917.

- (5) Brettel, K.; Leibl, W. *Biochim. Biophys. Acta* **2001**, *1507*, 100–114.
- (6) Hervas, M.; Ortega, J. M.; Navarro, J. A.; De la Rosa, M. A.; Bottin, H. *Biochim. Biophys. Acta* **1994**, *1184*, 235–241.
- (7) Sétif, P.; Bottin, H. *Biochemistry* **1995**, *34*, 9059–9070.
- (8) Nicholson, R. S.; Shain, I. *Anal. Chem.* **1964**, *36*, 706–723.
- (9) Cass, A. E. G.; Davis, G.; Francis, G. D.; Hill, H. A. O.; Aston, W. J.; Higgins, I. J.; Plotkin, E. V.; Scott, L. D.; Turner, A. P. F. *Anal. Chem.* **1984**, *56*, 6, 667–675.
- (10) Bourdillon, C.; Demaille, C.; Moiroux, J.; Savéant, J.-M. *J. Am. Chem. Soc.* **1993**, *115*, 2–10.
- (11) Heering, H. A.; Hirst, J.; Armstrong, F. A. *J. Phys. Chem.* **1998**, *102*, 6889–6902.
- (12) Hill, H. A. O.; Walton, N. J.; Whitford, D. *J. Electroanal. Chem.* **1985**, *187*, 109–119.
- (13) Kievit, O.; Brudvig, G. W. *J. Electroanal. Chem.* **2001**, *497*, 139–149.

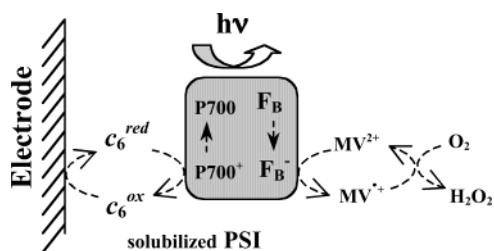


**Figure 1.** Light-driven electrocatalytic cycle showing electron flow from the electrode to  $O_2$ . Photosystem I (PSI) is schematized as two redox sites: the “donor” site, either in the reduced form (P700) or in the oxidized form (P700<sup>+</sup>), and the “acceptor” site, in the reduced ( $F_B^-$ ) or in the oxidized form ( $F_B$ ). The natural electron carrier, cyt  $c_6$  (oxidized,  $c_6^{ox}$ , or reduced,  $c_6^{red}$ ), is used at the donor site while a mediator (methyl viologen,  $MV^{2+}$ ) captures the electrons from  $F_B^-$ .

In this study, we take advantage of the fact that PSI, purified from *Thermosynechococcus elongatus*, has been stabilized in solution with the help of very low concentrations of detergent.<sup>14</sup> Thus, the two partners, solubilized PSI and cyt  $c_6$ , are in the bulk solution, and the catalytic reaction is treated as homogeneous (Figure 1). The PSI complex acts as a photooxidant of cyt  $c_6$ , and the electrocatalytic coupling is controlled by light. In contrast to the experimental conditions of flash spectroscopy measurements, electron transfers can be studied under steady-state conditions, that is, under continuous illumination.

One important prerequisite for the observation of electrocatalytic coupling is the direct and reversible electrochemistry of cyt  $c_6$  at the electrode interface in the appropriate scan rate range. From the pioneering works of several groups,<sup>15,16,17</sup> it is now generally accepted that the problems associated with the direct electrochemical investigation of redox proteins are either the passivation of the electrode by the irreversible adsorption of the protein onto the electrode surfaces or (and) inadequate protein purity in the sample. Modification of the electrode surface by self-assembly of a suitable promoter enhances the transfer rate and solves the first problem, and thus, most of the described metalloproteins (at least of small size) are now recognized as common electroactive species.

Recently purified and characterized, cyt  $c_6$  was not yet electrochemically studied on gold electrodes, and our first goal was to optimize the electrode modification to demonstrate the fast direct electrochemistry of this electron carrier. The next step was the detailed study of the light-driven transfer of electrons through the cyt  $c_6$ /PSI system using oxygen (and methyl-viologen) as terminal electron acceptor. Finally, the rate constants for the two limiting steps of the reaction, the cyt  $c_6$ /P700<sup>+</sup> and the  $F_B^-$ /methyl-viologen electron exchanges, were measured for the first time under steady-state conditions.

## Experimental Section:

**Materials.** Mercaptoethanol, 3-mercapto-1-propanol, 3-mercapto-propionic acid, mercapto-undecanoic acid, cysteamine, 4-aminothiophenol, ascorbic acid, 2-(6-dichlorophenol)indophenol, and methyl-viologen were purchased from Aldrich (Strasbourg, France).  $\beta$ -dodecyl maltoside ( $\beta$ -DM) and potassium ferricyanide were from Sigma (St Quentin Fallavier, France). Gold (purity 99.99%) was from Plateaxis (Noisy le

Sec, France). Organic solvents were HPLC grade. Water with a typical resistivity of 18 M $\Omega$  was from a Milli-Q purification system (Millipore, Les Ulis, France).

**Purifications of PSI and Cyt  $c_6$ .** PSI reaction centers from the cyanobacterium *Thermosynechococcus elongatus* were purified following Rögner et al.<sup>18</sup> (solubilization by 1% (w/v)  $\beta$ -DM, centrifugation on a sucrose density gradient, followed by anion exchange chromatography). The final stock solution of PSI contained 2 mg of chlorophyll/mL. The PSI concentration was determined using chlorophyll content with a ratio of 90 chlorophyll molecules for 1 PSI molecule, and the complex was maintained in solution with the help of 0.03%  $\beta$ -DM.

Cyt  $c_6$  from *Thermosynechococcus elongatus* was extracted and purified from cell free extract. The protein solution was first fractionated by stepwise ammonium sulfate precipitation. Then, fractions containing cyt  $c_6$  (precipitating at 3.6 M  $(NH_4)_2SO_4$ ) were purified by a combination of hydrophobic, anion exchange, and size exclusion HPLC chromatographies. Cyt  $c_6$  was spectrophotometrically found at >80% in the reduced state at the end of the purification. A stock solution of oxidized cyt  $c_6$  was prepared by oxidation with excess potassium ferricyanide followed by desalting on a Sephadex G25 column and concentration on Centricons 10 (Amicon). The final cyt  $c_6$  concentration of the stock solution was measured spectrophotometrically using an extinction coefficient of 24.4 mM<sup>-1</sup> cm<sup>-1</sup> at 552 nm for the reduced form and of 10 mM<sup>-1</sup> cm<sup>-1</sup> at 525 nm for the oxidized form.<sup>19,20</sup>

**Flash-Absorption Spectroscopy.** Kinetics of electron transfer from cytochrome  $c_6$  to PSI were also measured by flash spectroscopy at 820 nm as previously described.<sup>6</sup> The band-pass at 820 nm was 10 nm. From the kinetics of reduction of P700<sup>+</sup> by various concentrations of cyt  $c_6$ , pseudo first-order rate constants are determined as a function of cyt  $c_6$  concentration. These rate constants vary linearly with cytochrome concentration. The slope of the line is the bimolecular rate constant characterizing the electron transfer from reduced cyt  $c_6$  to photooxidized PSI (P700<sup>+</sup>). So, we calculated a rate constant of  $5.9 \pm 0.1 \times 10^6$  M<sup>-1</sup> s<sup>-1</sup>. The standard reaction mixture contained, in a final volume of 300  $\mu$ L, 5 mM Hepes buffer (pH 8), 50 mM Na<sub>2</sub>SO<sub>4</sub>, 5 mM MgSO<sub>4</sub>, 100  $\mu$ M methyl viologen, 2 mM Na-ascorbate, 0.03% (w/v)  $\beta$ -DM, an amount of purified PSI equivalent to 500  $\mu$ g chlorophyll/mL and 10 to 70  $\mu$ M cyt  $c_6$ .

Kinetics of electron transfer from the terminal acceptor of PSI to methyl viologen were measured by flash absorption spectroscopy at 500 nm (band-pass = 10 nm). These kinetics vary linearly with the methyl viologen concentration (studied in the range 50 to 400  $\mu$ M, in large excess to the PSI concentration), which allows for the derivation of a second-order rate constant of  $9 \pm 0.1 \times 10^6$  M<sup>-1</sup> s<sup>-1</sup>. The standard reaction mixture contained, in a final volume of 2 mL, 5 mM Hepes buffer (pH 8), 50 mM Na<sub>2</sub>SO<sub>4</sub>, 5 mM MgSO<sub>4</sub>, 2 mM Na-ascorbate, 27  $\mu$ M of 2-(6-dichlorophenol)indophenol, 0.03% (w/v)  $\beta$ -DM, an amount of purified PSI equivalent to 15  $\mu$ g chlorophyll/mL.

**Electrodes Preparation.** Au films (2  $\mu$ m thick) were made by vapor deposition (Edwards model 306) of gold on rigorously cleaned glass slides. Glass slides were cleaned in a boiling mixture of chloroform and methanol (2:1, v/v), followed by extensive water rinsing. Then, they were immersed in a freshly made chromic acid bath at 60 °C, rinsed in water, and dried under argon. The gold sheet was glued on the tip of a glass tube (3 mm in diameter, surface area  $S = 0.07$  cm<sup>2</sup>) in which a stainless steel wire was mounted. Conductive silver was used for electrical contact.

The gold interface was modified by chemisorption of various thiols. Just before modification of the gold surface, the electrodes were briefly cleaned in a fresh chromic acid solution and rinsed in water. The thiol monolayer was self-assembled by dipping the electrodes for 1 h into a

(14) Diaz-Quintana, A.; Navarro, J. A.; Hervas, M.; Molina-Heredia, F. P.; De la Cerda, B.; De la Rosa, M. A. *Photosynth. Res.* **2003**, *75*, 97–110.

(15) Eddowes, M. J.; Hill, H. A. O. *J. Am. Chem. Soc.* **1979**, *101*, 4461–4469.

(16) Taniguchi, I.; Toyosawa, K.; Yamaguchi, H.; Yasukouchi, J. *J. Electroanal. Chem.* **1982**, *140*, 187–194.

(17) Bowden, E. F.; Hawkrige, F. M.; Blount, H. N. *J. Electroanal. Chem.* **1984**, *161*, 355–362.

(18) Rögner, M.; Nixon P. J.; Diner B. A. *J. Biol. Chem.* **1991**, *265*, 6189–6196.

(19) Cho, Y. S.; Wang, Q. J.; Krogmann, D.; Whitmarsh, J. *Biophys. Biochim. Acta* **1999**, *1413*, 92–97.

(20) Cho, Y. S.; Pakrasi, H. B.; Whitmarsh, J. *Eur. J. Biochem.* **2000**, *267*, 1068–1074.

20 mM ethanolic solution of the substituted thiol. Finally, the modified electrodes were rinsed in ethanol and then water and were stored in standard buffer (5 mM HEPES pH 8, 50 mM Na<sub>2</sub>SO<sub>4</sub>, 5 mM MgSO<sub>4</sub>) until use.

**Electrochemical Measurements.** A Parstat 2263 potentiostat controlled by a PC computer and Power Suite software (Princeton Applied Research, Ametek, Trappes, France) was used for cyclic voltammetry experiments.

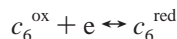
The electrochemical cell contained three electrodes: the working gold electrode, a platinum foil auxiliary electrode, and a KCl saturated calomel reference electrode (SCE = 0.245 V vs the normal hydrogen electrode at 20 °C). The working electrode was placed inside a microcell inserted in the center of the main electrochemical cell itself filled with 20 cm<sup>3</sup> of the buffer. The microcell was a simple glass tube of 4.0 mm inner diameter closed at the bottom with a glued dialysis membrane (MW cutoff 8 kDa). The biological sample, introduced into the microcell, was thus in electrical contact with the main cell through this membrane. The assembly allows working with small volumes (typically 50 to 100 μL) while avoiding uncontrolled ohmic drops. When needed, the cell was purged with argon or oxygen under gentle bubbling for 30 min. The temperature was kept at 20 °C by circulation of water in the jacket of the main cell.

For experiments in dark conditions, the electrochemical cell was covered with a black box. Illumination of the PSI solution with white light was provided in the electrochemical cell by an optical fiber system (Schott, KL1500, USA). The power of the incident light at the level of the PSI sample was measured at 300 μmol s<sup>-1</sup> m<sup>-2</sup>.

## Results and Discussion

**Direct Electrochemistry of Cytochrome *c*<sub>6</sub> from *Thermosynechococcus elongatus*.** Self-assembled monolayers of terminally derivatized thiols on gold electrodes have been shown to be efficient for the promotion of direct electrochemistry of small metalloproteins such as cytochrome *c*.<sup>21–23</sup> Reasonable electroactivity can be also obtained on untreated glassy carbon or pyrolytic graphite “edge” electrodes provided that the supporting electrolyte be specifically optimized, for example, by pH adjustment or addition of dications.<sup>24,25</sup>

On gold electrodes, the net charge of the protein is often evoked as a key parameter for the choice of the promoter molecule.<sup>26</sup> As the electrochemistry of cyt *c*<sub>6</sub> has been only described recently on pyrolytic graphite “edge” electrodes,<sup>27</sup> and not yet on gold electrodes, we have thus tested several thiols bearing different terminal groups in order to optimize the reversibility of the electrochemical reaction:



and also the long-term stability of cyt *c*<sub>6</sub> voltammetry.

The results presented in Table 1 are consistent with earlier literature data on metalloprotein electrochemistry. At pH 8, cyt *c*<sub>6</sub> exhibits a negative net charge (pH<sub>i</sub> calculated = 5.4). As

**Table 1.** Electrochemical Behavior of Cytochrome *c*<sub>6</sub> from *Thermosynechococcus elongatus* on Bare or Surface-Modified Gold Electrodes<sup>a</sup>

thiol monolayer on gold	formal potential <i>E</i> <sub>0</sub> (mV/NHE)	peak separation (mV) (at 10 mV s <sup>-1</sup> )	stability (1 day)
none	324	80–110	very unstable
mercaptopropionic acid		no peak	
mercaptoundecanoic acid		no peak	
cysteamine	321	70–90	unstable
aminothiophenol	327	70–75	stable
mercaptoethanol	326	85–90	unstable
mercaptopropanol	321	60–62	stable

<sup>a</sup> Cyclic voltammetry in HEPES buffer 5 mM, pH 8 + Na<sub>2</sub>SO<sub>4</sub> 50 mM + MgSO<sub>4</sub> 5mM.

expected, modification of the electrode surface with negative charges (here propionic and undecanoic acid) inhibited severely the electrochemical response. On the contrary, the grafting of a basic group (here cysteamine or aminothiophenol) resulted in a good reversibility. Even better reversibility and stability were obtained by using a neutral hydroxyl group (mercaptopropanol). As already discussed,<sup>23,28</sup> the short chain mercaptopropanol monolayer serves as an effective barrier to avoid protein adsorption and self-blocking of the gold interface.<sup>29</sup>

On several series of mercaptopropanol-modified gold electrodes and several cyt *c*<sub>6</sub> purification batches, the heterogeneous rate transfer constant, *k*<sub>s</sub>, was regularly measured between 0.5 × 10<sup>-2</sup> and 1.0 × 10<sup>-2</sup> cm s<sup>-1</sup> from the peak-to-peak potential using scan rates from 10 to 300 mV s<sup>-1</sup>. These data allowed the precise determination of both *E*<sub>0</sub> = 0.321 ± 0.005 V/NHE at pH 8, the formal potential of cyt *c*<sub>6</sub> in the experimental conditions and *D* = 1.2 × 10<sup>-6</sup> ± 0.2 × 10<sup>-6</sup> cm<sup>2</sup> s<sup>-1</sup>, the diffusion coefficient of cyt *c*<sub>6</sub>. The comparison given in Figure 2 between the experimental and the simulated curves at various scan rates demonstrates that the cyt *c*<sub>6</sub> couple behaves as expected in the theory of a quasi-reversible system.<sup>30,31</sup> It has to be noted that the value of *D* is in good agreement with the diffusion coefficient of globular proteins of similar molecular weight measured by ultracentrifugation.<sup>32</sup> In the literature, the diffusion coefficients of redox proteins are often underestimated by the electrochemical method.

**Light-Controlled Electrocatalytic Coupling between PSI and Cyt *c*<sub>6</sub>.** In a typical electrocatalytic experiment performed according to Figure 1, the oxidized form of cyt *c*<sub>6</sub> is introduced in solution together with methylviologen, oxygen (simply aerated solutions unless otherwise stated), and a catalytic amount of solubilized PSI (~0.25 μM unless otherwise stated). When the electrode potential is scanned cathodically, the reduced form of cyt *c*<sub>6</sub> is generated at the electrode surface and diffuses toward the bulk. In the dark, no catalytic reaction occurs and the recorded cyclic voltammetry signal solely corresponds to the reversible reduction of cyt *c*<sub>6</sub> (Figure 3, dark). Under illumination, the photogeneration of the (P700<sup>+</sup>, F<sub>B</sub><sup>-</sup>) pair triggers the

(21) Armstrong, F. A.; Hill, H. A. O.; Walton, N. *Acc. Chem. Res.* **1988**, *21*, 407–413.

(22) Taniguchi, I.; Toyosawa, K.; Yamaguchi, H.; Yasugouchi, K. *J. Chem. Soc., Chem. Commun.* **1982**, 1032.

(23) Terrataz, S.; Cheng, J.; Miller, C. J.; Guiles, R. D. *J. Am. Chem. Soc.* **1996**, *118*, 7857–7858.

(24) Armstrong, F. A.; Cox, P. A.; Hill, H. A. O.; Lowe, V. J.; Oliver, B. N. *J. Electroanal. Chem.* **1987**, *217*, 331–366.

(25) Szucks, A.; Novak, M. *J. Electroanal. Chem.* **1995**, *383*, 75–84. Szucks, A.; Novak, M. *J. Electroanal. Chem.* **1995**, *384*, 47–55.

(26) Rivera, M.; Wells, M. A.; Walker, F. A. *Biochemistry*, **1994**, *33*, 2161–2170.

(27) Dikiy, A.; Carpentier, W.; Vanderberghe, I.; Borsari, M.; Safarov, N.; Dikaya, E.; Van Beeumen, J.; Ciurli, S. *Biochemistry* **2002**, *41*, 14689–14699.

(28) Blankman, J. I.; Shahzad, N.; Dangi, B.; Miller, C. J.; Guiles, R. D. *Biochemistry* **2000**, *39*, 14799–14805.

(29) Hill, H. A. O.; Hunt, N. I.; Bond, A. M. *J. Electroanal. Chem.* **1997**, *436*, 17–25.

(30) Nicholson, R. S.; Shain, I. *Anal. Chem.* **1964**, *61*, 6663–6669.

(31) Bard, A. J.; Faulkner, L. R. In *Electrochemical Methods*; Wiley and Sons: New York, 1980; pp 213–248.

(32) In *Handbook of Biochemistry*; Sober, H. A., Ed.; CRC Press: Cleveland, 1970.



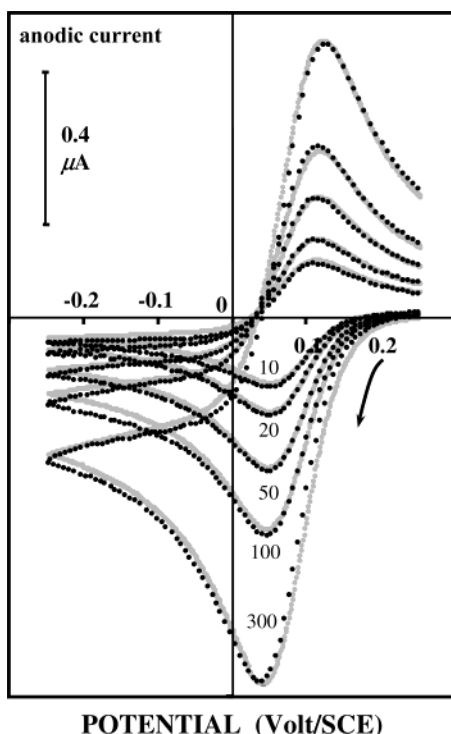


**Figure 2.** Cyclic voltammetry at various scan rates (10, 20, 50, 100, 300  $\text{mV s}^{-1}$ ) of cyt *c*<sub>6</sub> in the oxidized form (87  $\mu\text{M}$  in HEPES buffer 5 mM, pH 8 +  $\text{Na}_2\text{SO}_4$  50 mM +  $\text{MgSO}_4$  5 mM). The electrode was previously modified by chemisorption of mercaptopropional on the gold interface. Black points (●): experimental data, corrected from background currents. In gray, simulated curves calculated for the five scan rates with the following parameters:  $E_0 = 0.080$  V/SCE (0.321 V/NHE);  $S = 0.07$   $\text{cm}^2$ ;  $D = 1.2 \times 10^{-6}$   $\text{cm}^2 \text{s}^{-1}$ ;  $k_s = 7 \times 10^{-3}$   $\text{cm s}^{-1}$ ; 20 °C.

catalytic cycle. This results in the regeneration of  $c_6^{\text{ox}}$  thus yielding an increase of the cathodic current. As shown in Figure 3, the shape of the signal also changes drastically: from peak shaped in the dark, the voltammogram becomes S-shaped under illumination. This behavior demonstrates the efficient coupling between the reversible electrochemistry of cyt *c*<sub>6</sub> at the electrode and its reaction with PSI in solution. The very occurrence of a plateau current also indicates that the overall catalytic process is fast compared to diffusion and also shows that the consumption of  $\text{MV}^{2+}$  during the time of a voltammogram is negligible.<sup>10,33,34</sup> Following the same idea, any increase in the scan rate reduces the catalytic efficiency. Here the catalytic current becomes negligible when the scan rate is increased up to 2 V  $\text{s}^{-1}$  (not shown).

The parameters controlling the electrocatalytic path were systematically studied. Further evidence that the cathodic current originates from the photocatalytic reaction induced by turnover of PSI comes from its dependence on the intensity of illumination (Figure 3). For a convenient control of the light intensity, several neutral density filters were placed between the electrochemical cell and the illumination device. As expected, the electrocatalytic process was controlled by light intensity and exhibits a typical saturation behavior (Figure 3, inset). Numerous other control experiments demonstrate that (i) the omission of

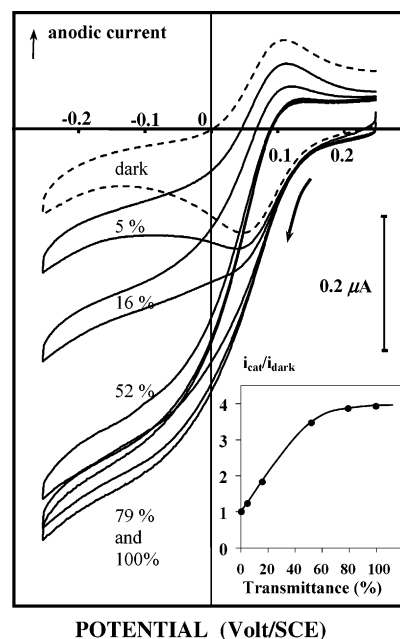


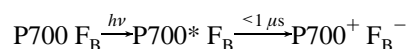
**Figure 3.** Typical behavior of electrocatalytic coupling when the light intensity is increased up to PSI saturation (voltammograms at 10  $\text{mV s}^{-1}$  not corrected from background). PSI = 0.25  $\mu\text{M}$ ; cyt *c*<sub>6</sub> = 50  $\mu\text{M}$ ; methylviologen = 200  $\mu\text{M}$  in aerated HEPES buffer 5 mM, pH 8 +  $\text{Na}_2\text{SO}_4$  50 mM +  $\text{MgSO}_4$  5 mM. The broken line gives the cyt *c*<sub>6</sub> voltammogram without catalysis (dark). The light intensity was controlled by four neutral density filters: 5%, 16%, 52%, and 79%. The inset shows the light saturation curve for the catalytic efficiency:  $i_{\text{cat}}/i_{\text{dark}}$ , where  $i_{\text{cat}}$  is the plateau current (here at  $-0.2$  V) and  $i_{\text{dark}}$  is the cyt *c*<sub>6</sub> peak current without catalysis.

one component like cyt *c*<sub>6</sub>, PSI,  $\text{O}_2$ , or  $\text{MV}^{2+}$  suppresses the catalysis; (ii) the catalytic current is related to the PSI concentration as expected; and (iii) the voltammograms do not significantly change if a pure oxygen atmosphere is introduced in the place of air. This demonstrates that the homogeneous reaction between reduced viologen and  $\text{O}_2$  is sufficiently fast for there to be no time for reduced viologen to be significantly electrochemically oxidized at the electrode surface.

As the catalytic current was found related to the initial concentrations of cyt *c*<sub>6</sub> and  $\text{MV}^{2+}$ , information about the kinetics of the catalytic cycle can be extracted from the study of the S-shaped voltammogram most conveniently by measuring the intensity of its plateau current.

**Kinetics of the Electron-Transfer Reactions between PSI and Both  $\text{MV}^{2+}$  and Cyt *c*<sub>6</sub>.** The overall catalytic reaction rate can be related to the individual steps of the catalytic cycle depicted on Figure 1 provided that a detailed mechanism is postulated. Such a mechanism is presented on Figure 4 and relies on the following assumptions.

First, the charge separation, resulting from the photo-generation of the ( $\text{P700}^+$ ,  $\text{F}_B^-$ ) pair is represented by a first-order reaction with rate constant  $k_1$ . This reaction is not an elementary step as it corresponds to the absorption of a photon followed by electron transfer within the PSI complex to give complete charge separation according to the following scheme:



The internal electron transfer being very fast ( $>10^6$   $\text{s}^{-1}$ ),<sup>5</sup> the apparent kinetics of formation of the charge separated state under continuous illumination is limited by the light absorption

(33) Savéant, J. M.; Vianello, E. In *Advances in Polarography*; Langmuir I. S., Ed.; Pergamon Press: London, 1960; Vol. 1, pp 367–374.

(34) Andrieux, C. P.; Savéant, J.-M. In *Electrochemical Reaction in Investigation of Rates and Mechanisms of Reactions, Techniques of Chemistry*; Bernasconi, C. F., Ed.; Wiley: New York, 1986; Vol. VI/4E, Part 2, pp 305–390.

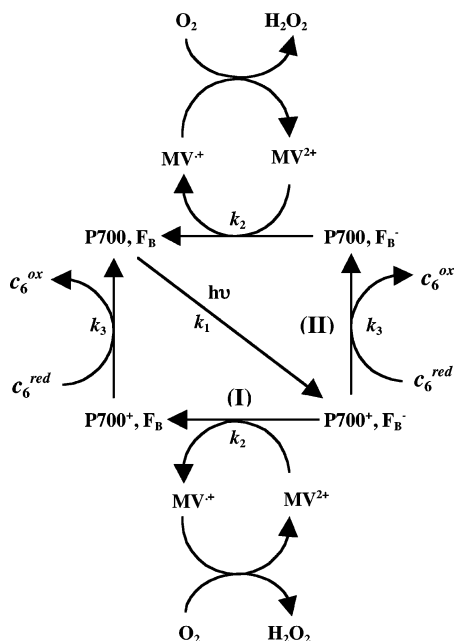


**Figure 4.** Schematic view of the proposed mechanism for electron exchange between PSI, cyt  $c_6$ , and  $MV^{2+}$ . Path I and path II are distinguished by the order of successive PSI oxidation or reduction steps with the two electron carriers.

and the fraction of PSI with P700 in the photochemically active neutral (ground/reduced) state.<sup>35</sup>

Second, once charge separation is complete, the  $(P700^+, F_B^-)$  complex can be either first oxidized by  $MV^{2+}$  (path I) or reduced by  $c_6^{red}$  (path II). As these reactions proceed at comparable rates (see below), both paths have to be considered. They are assumed to be irreversible as they are both thermodynamically very favorable.<sup>35</sup>  $\Delta E = +0.17$  V for the reduction of  $P700^+$  by  $c_6^{red}$ <sup>36</sup> and + 0.2 V for the oxidation of  $F_B^-$  by  $MV^{2+}$ .<sup>37</sup> Moreover, they are followed by reactions faster than their return step (uphill).

Third assumption: the oxygen concentration is high enough, and thus the oxidation of reduced viologen by oxygen is assumed to be fast enough not to interfere with the overall catalytic rate. This implies that the regeneration of  $MV^{2+}$  is very effective and therefore that its consumption during the catalytic cycle is negligible. Thus, we consider that at any time,  $[MV^{2+}] = C_{MV}^0$ , the initial methyl-viologen concentration.<sup>38</sup>

Applying the steady-state approximation to PSI in each of its redox states ( $(P700, F_B)$  pairs) yields the following rate law:<sup>39</sup>

$$V_{cat} = \frac{k_3 C_6^{red} [PSI]}{1 + k_3 C_6^{red} \left\{ \frac{1}{k_1} + \frac{1}{k_2 C_{MV}^0 (1 + k_2 C_{MV}^0 / k_3 C_6^{red})} \right\}}$$

$V_{cat}$  being the overall catalytic rate,  $C_6^{red}$ , the reduced cyt  $c_6$  concentration, and  $[PSI]$ , the total PSI concentration.

(35) We can estimate, from Brettel et al.,<sup>5</sup> the recombination rates of the pair  $(P700^+, F_B^-)$  to be in the range of some tens of milliseconds, which is slower than the millisecond time scale of the electron-transfer reactions between PSI and both  $MV^{2+}$  and cyt  $c_6$  considered in this study.

(36) Sétif, P.; Mathis, P. *Arch. Biochem. Biophys.* **1980**, *204*, 477–485.

(37) Ke, B.; Hansen, R. E.; Beinert, H. P. *Proc. Natl. Acad. Sci. U.S.A.* **1973**, *70*, 2941–2945.

(38) The validity of this latter point was experimentally ascertained by observing that, as described in the text, a plateau shaped catalytic signal was always obtained. Moreover, increasing the oxygen concentration by saturating the solution with oxygen instead of ambient air yielded only a small increase of catalysis.

During the course of the voltammogram, the diffusion/reaction of  $c_6^{red}$  is described by Fick's second law as

$$\frac{\partial C_6^{red}}{\partial t} = D \frac{\partial^2 C_6^{red}}{\partial x^2} - V_{cat} \quad (1)$$

$D$  being the diffusion coefficient of cyt  $c_6$ ,  $t$ , the time variable, and  $x$ , the distance away from the electrode surface.

And, the current is given by

$$i = -FS D \left( \frac{\partial C_6^{red}}{\partial x} \right)_{x=0} \quad (2)$$

$S$  being the electrode area, and  $F$ , the Faraday constant.

Complete resolution of the diffusion/reaction problem, leading to the calculation of the current–potential curves, can be carried out using simulation techniques such as those previously reported.<sup>10,33,34,40</sup>

However, provided that the catalytic cycle is fast enough (or equivalently, the scan rate slow enough), S-shaped voltammograms are always obtained. An analytical expression of the plateau current of these “purely catalytic” voltammograms can be derived by integrating eq 1, as the occurrence of such a plateau corresponds to  $(\partial C_6^{red} / \partial t) = 0$ .

The two required boundary conditions are given by (i)  $C_6^{red} = 0$  for  $x \rightarrow +\infty$  (no reduced cyt  $c_6$  present in solution) and (ii) at the potentials where the plateau occurs,  $C_6^{red}$  at the electrode surface =  $C_6^0$  the initial cyt  $c_6$  concentration.

From eq 2, one then derives the following expression for the plateau current:

$$i_{cat} = FS \sqrt{DC_6^{red}} \sqrt{k_{app} [PSI]}$$

with  $k_{app}$  an apparent second-order rate constant for PSI reduction by cyt  $c_6$  (see below).

In terms of catalytic efficiency, that is to say the ratio of the plateau current measured in the presence of catalysis (which means with illumination) to the “dark current”  $i_{dark}$  measured within the same solution but in the absence of catalysis, this translates into the simple expression:<sup>10</sup>

$$\frac{i_{cat}}{i_{dark}} = 2.24 \sqrt{\frac{RT[PSI]}{Fv}} k_{app} \quad (3)$$

$v$  being the potential scan rate.

The apparent second-order rate constant  $k_{app}$  is related to the rate constants of the individual steps of the mechanism

(39) According to the method of Kruijff, J. et al., *Photosynthesis Research*, **1994**, *40*, 279–286, PSI is here purified in a trimeric form of about 1000 kDa. This complex being a much larger molecule than any of the other reactants its diffusion was not taken into account, and a purely “chemical” steady-state approximation was applied to all of its redox forms. The very low concentration of PSI also implies that its turnover is very large during the time course of a voltammogram and thus ensures that its redox forms are continuously at steady state. By a very rough calculation, starting from a catalytic current of some 300 nA and considering a reaction layer of some 10  $\mu\text{m}$  thick, containing around  $10^{10}$  PSI molecules, we arrive at a turnover number per PSI molecule of some 200  $\text{s}^{-1}$ .

(40) The DigiSim simulation package was also used to simulate the voltammograms in the most general cases. Although this program requires entering a large number of parameters, the exact values of which being often unknown, it allowed us to validate some of the simplifying assumptions used in this work.

presented in Figure 4 by the following:

for  $\rho > 3\sigma$ ,

$$k_{\text{app}} = \frac{2k_3}{\rho + \sigma} \left\{ 1 + [(\rho + \sigma)(\rho - 3\sigma)]^{-1/2} \ln \left( \frac{2 + \rho + \sigma - \sqrt{(\rho + \sigma)(\rho - 3\sigma)}}{2 + \rho + \sigma + \sqrt{(\rho + \sigma)(\rho - 3\sigma)}} \right) \right\}$$

for  $\rho < 3\sigma$ ,

$$k_{\text{app}} = \frac{2k_3}{\rho + \sigma} \left\{ 1 - 2[(\rho + \sigma)(\rho - 3\sigma)]^{-1/2} \left[ \tan^{-1} \left( (2\sigma + 1) \sqrt{\frac{\rho + \sigma}{3\sigma - \rho}} \right) - \tan^{-1} \left( \sqrt{\frac{\rho + \sigma}{3\sigma - \rho}} \right) \right] \right\} \quad (4)$$

and for  $\rho = 3\sigma$ ,

$$k_{\text{app}} = \frac{4k_3\sigma}{(\rho + \sigma)(1 + 2\sigma)}$$

with  $\sigma = k_3 C_6^0/k_2 C_{\text{MV}}^0$  and  $\rho = k_3 C_6^0/k_1$ .

The dimensionless parameter  $\sigma$  compares the reduction rate of PSI by cyt *c*<sub>6</sub> to its oxidation rate by methyl-viologen. The level of this parameter also decides which path (I or II) is predominantly followed by the catalysis. The dimensionless parameter  $\rho$  compares the rate of PSI reduction by cyt *c*<sub>6</sub> to the generation rate of the (P700<sup>+</sup>, F<sub>B</sub><sup>-</sup>) pair. In the general case, the catalytic efficiency depends on  $k_3$ ,  $\sigma$ , and  $\rho$ .

The reliability of this theoretical analysis was checked on various experimental situations, and a typical comparison with the experiment is given on Figure 5.

**Electrochemical Determination of  $k_3$  and  $k_2$ .** The independent determination of the rate constant  $k_3$  can only be carried out when  $\sigma \rightarrow 0$  and  $\rho \rightarrow 0$  as we can see from the above equations that we then have  $k_{\text{app}} = k_3$ . From the definition of the above parameters, it follows that such a limiting case situation can be met when  $C_6^0 \rightarrow 0$ . Physically, this situation corresponds to the cyt *c*<sub>6</sub> concentration being sufficiently low for the reduction of P700<sup>+</sup> by  $C_6^{\text{red}}$  to become the rate determining step (the rate law then simplifies to  $V_{\text{cat}} = k_3 C_6^{\text{red}} [\text{PSI}]$ ). A convenient diagnosis criterion that this “pseudo-first-order” situation has been reached is that the catalytic efficiency then ceases to depend on the concentration of cyt *c*<sub>6</sub>. Experimentally, we observed that this occurred when  $C_6^0 \leq 50 \mu\text{M}$  (working with  $C_{\text{MV}}^0 \geq 200 \mu\text{M}$ ). For such low cyt *c*<sub>6</sub> concentrations, from the catalytic efficiency determined at the plateau of the S-shaped voltammogram recorded at a slow scan rate (10 mV/s), we obtained (using eq 3)  $k_3 = 6 \pm 0.5 \times 10^6 \text{ M}^{-1} \text{ s}^{-1}$ . This value is in agreement with that derived from laser-flash experiments:  $k_3 = 5.9 \pm 0.1 \times 10^6 \text{ M}^{-1} \text{ s}^{-1}$  (see Experimental Section). It shows that there is no additional limiting step in PSI reduction by cyt *c*<sub>6</sub>. Such a step (for example, dissociation of oxidized cyt *c*<sub>6</sub> following its transient binding to PSI) would slow the continuous turnover of the system and decrease the  $k_3$  value determined electrochemically. The absence of any detectable binding of cyt *c*<sub>6</sub> on PSI has been observed in the cyanobacterium *Synechocystis* sp PCC 6803<sup>6</sup> and also in *Thermosynechococcus elongatus* (present work).

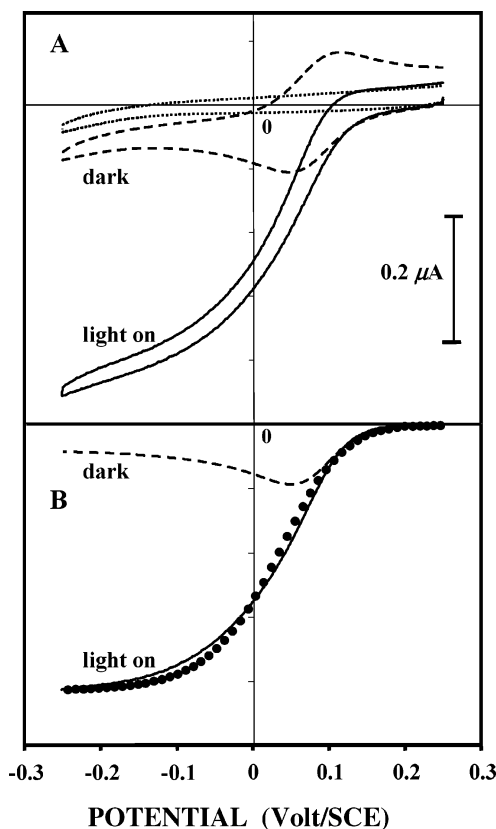


**Figure 5.** Light-triggered, PSI-catalyzed reduction of methyl-viologen by cyt *c*<sub>6</sub>. (A) Experimental cyclic voltammograms at 10 mV s<sup>-1</sup> for thiol-modified electrode background without cyt *c*<sub>6</sub> (dotted line); catalytic solution in the dark (broken line); and catalytic solution under illumination at saturation (continuous line). The solution contains PSI = 0.25 μM; cyt *c*<sub>6</sub> = 50 μM; methyl-viologen = 800 μM in aerated Hepes buffer 5 mM, pH 8 + Na<sub>2</sub>SO<sub>4</sub> 50 mM + MgSO<sub>4</sub> 5 mM. (B) Comparison of background-subtracted cathodic scan curve (continuous line) with a theoretical catalytic voltammogram (●). The simulation was made according to eqs 3 and 4 using the following parameters (defined in the text):  $\sigma = 0.3$ ,  $\rho = 0$ . The values of  $k_3 = 8.6 \times 10^{-3} \text{ cm s}^{-1}$  and  $D = 1 \times 10^{-6} \text{ cm}^2 \text{ s}^{-1}$  were determined at this particular electrode ( $S = 0.07 \text{ cm}^2$ ) from the fitting with the experimental voltammogram in the dark (broken line).

Starting from such a pseudo-first-order situation, where  $\rho \ll 1$  and  $\sigma \ll 1$ , we then lowered the methyl-viologen concentration  $C_{\text{MV}}^0$  to below 200 μM. This results in increasing  $\sigma$  while  $\rho$  is kept low.<sup>41</sup> Therefore, the apparent rate constant is then given by the following expression derived from eq 4 when  $\rho \ll 1$ :

$$k_{\text{app}} = \frac{2k_2 C_{\text{MV}}^0}{C_6^0} \left( 1 - \frac{2k_2 C_{\text{MV}}^0}{\sqrt{3} k_3 C_6^0} \left[ \tan^{-1} \left( \frac{1 + 2k_3 C_6^0/k_2 C_{\text{MV}}^0}{\sqrt{3}} \right) - \pi/6 \right] \right) \quad (5)$$

As a result,  $k_3$  being known, the value of  $k_{\text{app}}$  depends only on  $k_2$  and on the methyl-viologen “excess” ratio defined as  $C_{\text{MV}}^0/C_6^0$ . The lower this ratio, the lower  $k_{\text{app}}$  and the less intense the catalysis. Keeping  $C_6^0$  at 50 μM and reducing  $C_{\text{MV}}^0$  to 50 μM, we indeed observed the expected decrease in the catalysis efficiency (see Figure 6).<sup>42</sup> It is noteworthy that even in this

(41) The experimentally observed saturation of the catalytic current with increasing light intensity shows that, under saturating conditions, the charge separation step does not participate in the kinetic control of the catalytic cycle. Within the framework of the kinetic model proposed here, this translates into  $\rho$  being negligible.

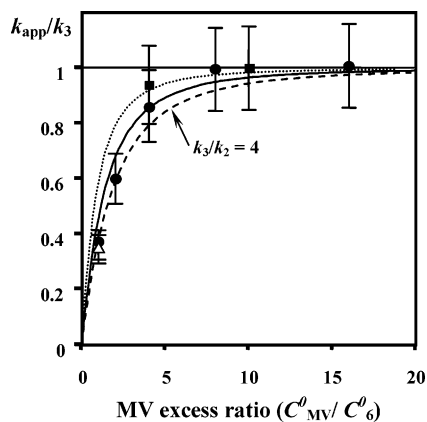


**Figure 6.** Evaluation of  $k_2$ : variation of the apparent rate constant  $k_{app}$  for PSI reduction by cyt  $c_6$  as a function of the methyl-viologen excess ratio defined as  $C_{MV}^0/C_6^0$ .  $k_{app}$  is normalized by  $k_3 = 6 \times 10^6 \text{ M}^{-1} \text{ s}^{-1}$ , which was determined as described in the text. Each type of symbol corresponds to a set of experiments conducted as follows. (■)  $C_{MV}^0 = 200 \mu\text{M}$ ,  $C_6^0 = 50$  and  $20 \mu\text{M}$ ,  $[\text{PSI}] = 0.25 \mu\text{M}$ . (●)  $C_6^0 = 50 \mu\text{M}$ ,  $C_{MV}^0$  varying from 50 to  $800 \mu\text{M}$ ,  $[\text{PSI}] = 0.25 \mu\text{M}$ . (Δ)  $C_6^0 = 50 \mu\text{M}$ ,  $C_{MV}^0 = 50 \mu\text{M}$ ,  $[\text{PSI}] = 0.5 \mu\text{M}$ . The error bars correspond to a 15% error on the  $k_{app}/k_3$  ratio. The dotted, continuous, and dashed lines are calculated using eq 5, and values of 2, 3, and 4, respectively, for the  $k_3/k_2$  ratio.

case an S-shaped catalytic signal was obtained (not shown). This demonstrates that the oxidized methyl-viologen concentration in the vicinity of the electrode is maintained at a constant value by the rapid oxidation of  $\text{MV}^+$  by oxygen. However, to keep a sufficiently high catalytic efficiency even at the lowest methyl-viologen concentration explored, the PSI concentration had to be raised to  $0.5 \mu\text{M}$ .

The values of  $k_{app}$  determined using eq 3 for several values of the  $C_{MV}^0/C_6^0$  ratio are presented in Figure 6. As expected, when this ratio is high (methyl-viologen is then in excess)  $k_{app}$  tends toward  $k_3$ . When the methyl-viologen excess ratio is decreased to less than  $\sim 4$ ,  $k_{app}$  decreases sharply. This variation in  $k_{app}$  with the methyl-viologen excess can be fitted using eq 5 once a value is given for  $k_2$  or, equivalently, for the  $k_3/k_2$  ratio. The best fit of the data points is shown in Figure 6 for a value of  $k_3/k_2 = 3 \pm 1$  which leads to  $k_2 = 2 \pm 1 \times 10^6 \text{ M}^{-1} \text{ s}^{-1}$ . The value determined in parallel by flash absorption spectroscopy was of the same order of magnitude but higher ( $k_2 = 9 \times 10^6 \text{ M}^{-1} \text{ s}^{-1}$ ; see Experimental Section). A possible explanation for this discrepancy is that the two measurements were performed under different operating conditions for PSI.

Conceptually, flash adsorption spectroscopy uses a single PSI turnover while voltammetry exploits steady-state conditions. This could result in different relative weights for the possible side reactions interfering with the measurements such as direct reduction of cyt  $c_6$  by reduced viologen, dimerization, or electrochemical oxidation of reduced viologen.

## Conclusion

The use of a solubilized PSI, purified from a cyanobacterium, allowed the development of a new example of “homogeneous” enzymatic electrocatalysis.<sup>43</sup> In this special case, the electrocatalytic coupling was controlled by light through an artificial photosynthetic electron-transfer chain which carried the electrons from the electrode to oxygen. This artificial chain was able to photogenerate electrons at low potential under steady-state conditions, and the resulting catalytic current was found to be stable for hours.

On the mechanistic point of view, we have shown that, provided a comprehensive kinetic scheme describing the fate of the  $(\text{P700}^+, \text{F}_B^-)$  pair generated by illumination of PSI is established, the steady-state kinetics of both the reduction and the oxidation of PSI by soluble cofactors can be investigated in unison by cyclic voltammetry. The plateau current of the catalytic voltammogram is related by simple analytic expressions to the rate constants of the reactions involved in the catalytic cycle. Studying the variation of this plateau current as a function of the reactant concentrations thus allows the identification of limiting cases from which the values of the individual rate constants of the oxidation and of the reduction reaction of PSI can be determined. The reasonable agreement between the values for these rate constants, determined here under stationary conditions, and the values reported in the literature validates the electrochemical approach to studying photocatalyzed electron-transfer reactions.

**Acknowledgment.** We are grateful to Ms. Véronique Mary for expert technical assistance and to Dr. Alain Boussac for generous gifts of *Thermosynechococcus elongatus* protein extracts.

JA0363819

- (42) As the methyl-viologen concentration is lowered, it is legitimate to worry that  $\text{O}_2$  could start competing with  $\text{MV}^{2+}$  to act as an electron acceptor for  $\text{F}_B^-$ . To rule out this possibility, control experiments were carried out in the absence of  $\text{MV}^{2+}$ : no catalysis was observed in this case.
- (43) Bourdillon, C.; Demaille, C.; Moiroux, J.; Savéant, J.-M. *Acc. Chem. Res.* **1996**, *29*, 529–536.